

Transient phonon vacuum squeezing due to femtosecond-laser-induced bond hardeningFairoja Cheenicode Kabeer,^{*} Naira S. Grigoryan, Eeuwe S. Zijlstra, and Martin E. Garcia*Theoretische Physik, Universität Kassel and Center for Interdisciplinary Nanostructure Science and Technology (CINaT),
Heinrich-Plett-Straße 40, 34132 Kassel, Germany*

(Received 20 December 2012; revised manuscript received 9 July 2014; published 15 September 2014)

Ultrashort optical pulses can be used both to create fundamental quasiparticles in crystals and to change their properties. In noble metals, femtosecond lasers induce bond hardening, but little is known about its origin and consequences. Here we simulate ultrafast laser excitation of silver at high fluences. We compute laser-excited potential-energy surfaces by all-electron *ab initio* theory and analyze the resulting quantum lattice dynamics. We also consider incoherent lattice heating due to electron-phonon interactions using the generalized two-temperature model. We find phonon hardening, which we attribute to the excitation of *s* electrons. We demonstrate that this may result in phonon vacuum squeezed states with an optimal squeezing factor of ~ 0.001 at the *L*-point longitudinal mode. This finding implies that ultrafast laser-induced bond hardening may be used as a tool to manipulate the quantum state of opaque materials, where, so far, the squeezing of phonons below the zero-point motion has only been realized in transparent crystals by a different mechanism. On the basis of our finding, we further propose a method for directly measuring bond hardening.

DOI: [10.1103/PhysRevB.90.104303](https://doi.org/10.1103/PhysRevB.90.104303)

PACS number(s): 78.47.J-, 63.20.dk, 71.20.Be, 63.20.kd

I. INTRODUCTION

Vacuum squeezing is a fundamental quantum-mechanical effect involving a state in which the uncertainty in one of two conjugate variables drops below that of the vacuum state. It can be mathematically characterized by a nonpositive Glauber-Sudarshan *P* distribution [1] or by a positive squeezing factor [2]. At finite temperatures, the variance of thermal motions may also be squeezed, i.e., so-called thermal squeezing [3,4], which can be described either quantum mechanically or in the classical approximation, where the most appropriate description depends on the lattice temperature. Near 0 K, vacuum squeezing may be induced. In this case, a quantum-mechanical description is essential. Vacuum squeezing as such has no classical analog.

Strongly squeezed photons with squeezing factors close to 1 (Ref. [5]) find applications in the fields of quantum communication [6] and gravitational wave detection [7,8]. A variety of squeezed states has been proposed for other bosons, in particular, those associated with atomic vibrations in quantum dots [9,10], quantum wells [11,12], molecules [13,14], and polaritons [15,16]. In crystals, the excitation and measurement of squeezed phonons can be of great importance for fundamental explorations and for studying the ultrafast dynamics of excited states on atomic length scales [17,18]. However, this effect is hard to achieve due to the weak coupling of light with lattice vibrations and relatively strong incoherent electron-phonon interactions.

In recent decades, it has been shown that in transparent solids, femtosecond-laser excitation can lead to a vacuum squeezed phonon state via second-order Raman scattering [2,19,20]. The same phenomenon has not yet been demonstrated in opaque materials. Recently, *thermally* squeezed states have been observed in bismuth [21] and germanium [22] opaque crystals, as a consequence of laser-induced

bond softening. In these systems, the variance of the atomic displacements increases above that of the vacuum state [21,22].

In the present study, we theoretically explore the possibility of generating vacuum squeezed longitudinal phonons at different points in the Brillouin zone (BZ) of silver (point group O_h), which is shown in the inset of Fig. 1. In contrast to semimetals, Ag shows bond hardening after ultrashort-laser excitation [23] (Sec. II), but its influence (Sec. III) is counteracted by incoherent electron-phonon coupling (Sec. IV). Here, we add both effects in order to establish the conditions under which the bond hardening wins and phonon vacuum squeezing results (Sec. V).

II. ORIGIN OF BOND HARDENING

Recent theoretical [23] and experimental [24] studies on noble metals predict a hardening of phonon modes after electronic excitation on extremely short time scales, i.e., shorter than the equilibration between the excited electrons and the lattice, which lasts picoseconds [25]. Figure 1 shows this effect for the longitudinal *L*- and *X*-point phonons in silver. Since the lattice vibrational frequencies have changed after excitation, the system no longer evolves in the ground-state potential and a perturbing potential arises from the atomic displacements. In particular, the atomic motions along longitudinal phonon directions cause the overlap of electronic distributions between neighboring atoms to increase. As a result, the bands broaden and the electronic density of states (DOS) changes. In order to quantify these changes, we computed the DOS of silver in the ground state with and without atomic displacements along a longitudinal phonon direction [Fig. 2(a)]. In both cases, a high DOS peak between -6.5 and -2.5 eV below the Fermi level arising from the *4d* electrons is superimposed on a lower and broader distribution starting at -8 eV belonging to the half-filled *5s* band. Figure 2(b) shows the difference in the DOS in the central region of the *s* band. The negative difference in the DOS indicates that electrons in the *5s* band are distributed

^{*}fairu.ck@gmail.com

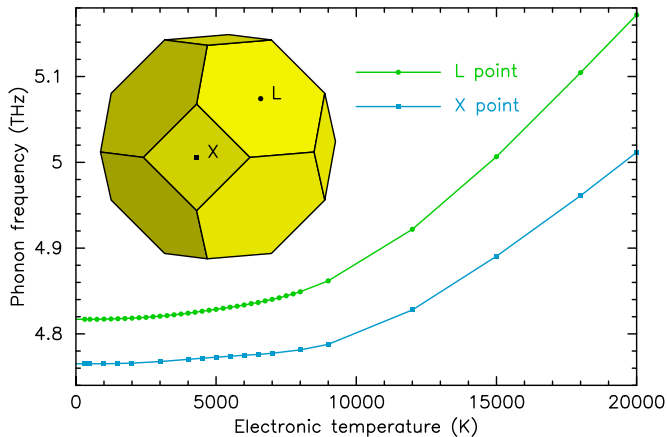


FIG. 1. (Color online) *Ab initio* computed longitudinal *L*- and *X*-point phonon frequencies in femtosecond-laser excited silver as a function of the laser-induced electronic temperature. Inset: The Brillouin zone of silver.

over a wider energy range, away from the Fermi energy, when the atoms are displaced.

Figure 3 schematically illustrates the phonon potential energy: Before laser excitation, one observes a parabola whose second derivative is proportional to the square of the phonon frequency. After femtosecond-laser excitation, the atoms move on a laser-excited potential-energy surface, *viz.*, Mermin's free energy of the electrons at a constant high electronic temperature T_e . The relationship between the ground-state potential-energy surface and the laser-excited phonon potential can be approximately described by a Sommerfeld expansion [26],

$$U(T_e) \approx U(0) - \frac{\pi^2}{6} (k_B T_e)^2 \text{DOS}(E_F), \quad (1)$$

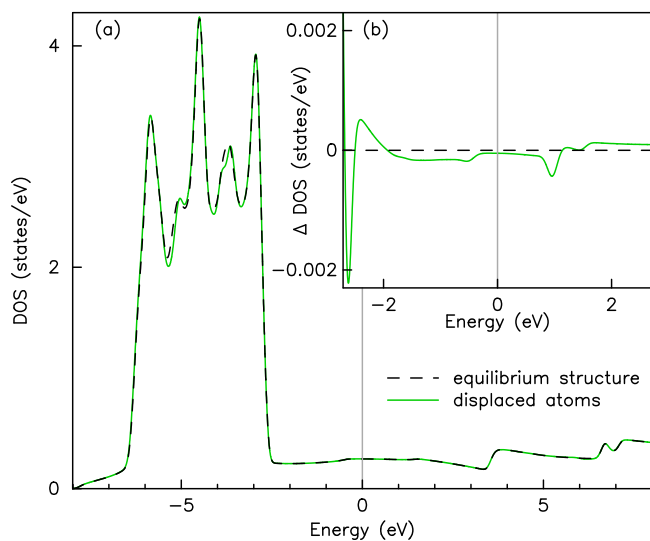


FIG. 2. (Color online) (a) Electronic ground-state DOS of silver without (black dashed line) and with (green solid line) atomic displacements in the direction of the *L*-point longitudinal phonon mode. (b) Difference in DOS around the center of the half-filled 5s band. Gray vertical lines indicate the Fermi energy.

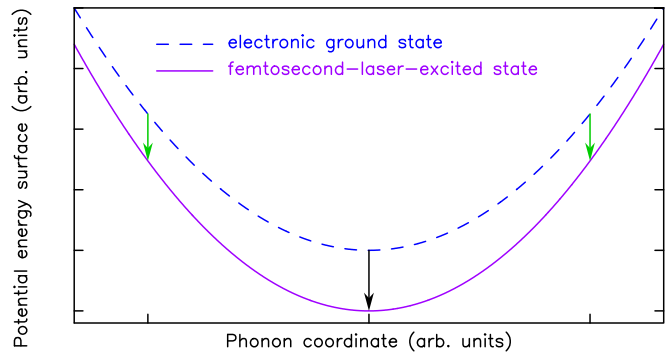


FIG. 3. (Color online) Schematic illustration of Mermin's free-energy change after laser excitation for the phonon mode whose electronic DOS is shown in Fig. 2.

where k_B is Boltzmann's constant and $\text{DOS}(E_F)$ is the electronic DOS at the Fermi energy. Because of the smaller electronic DOS at finite displacement, Mermin's free energy decreases less with increasing displacement after laser excitation, leading to a steepening of the potential energy versus displacement. This is the origin of bond hardening in noble metals at electronic temperatures $T_e \sim 2000\text{--}8000$ K, on which our present study is focused. Our result that the excitation of 5s electrons dominates the phonon hardening is in agreement with the finding of Ref. [27], where at these electronic temperatures, the electronic structure of noble metals resembles the free-electron gas model, where only the *s*-band electrons overlap.

At higher T_e , a significant amount of *d*-band electrons is additionally excited, which—we found—contributes also to the bond hardening at very high fluences [28]. It is interesting to note that these two physical mechanisms are both different from the origin of bond softening and hardening in Mg, which are related to the appearance of new Van-Hove singularities in the electronic DOS, when the atoms are displaced [26].

III. COHERENT EFFECT OF BOND HARDENING

In bond-softening materials, for example, semiconductors and semimetals [29,30], the laser-induced potential is shallower than in the electronic ground state. Therefore, the phonon wave function, whose width is at sufficiently low lattice temperature initially equal to the zero-point motion $\langle Q_{\mathbf{q}\lambda}^2 \rangle_{0\text{K}}$ and which is afterwards characterized by the expectation value $\langle Q_{\mathbf{q}\lambda}^2(t) \rangle$, where $Q_{\mathbf{q}\lambda}$ is the normal coordinate of the phonon with wave vector \mathbf{q} and branch index λ , is too narrow, immediately following the femtosecond-laser pulse, for the laser-modified potential. So it starts to broaden in an oscillatory fashion as follows from the time-dependent Schrödinger equation. After a quarter of a phonon period, the wave-packet expands in real space, *i.e.*, its mean-square width, reaches a maximum and, after half a phonon period, the wave packet reaches its minimum width, which, however, is not narrower than the initial state. Therefore, the squeezing factor

$$S = 1 - \sqrt{\frac{\langle Q_{\mathbf{q}\lambda}^2(t) \rangle}{\langle Q_{\mathbf{q}\lambda}^2 \rangle_{0\text{K}}}}, \quad (2)$$

with respect to the 0K mean-square width before laser excitation, $\langle Q_{\mathbf{q}\lambda}^2 \rangle_{0\text{K}} = \hbar/2M\omega_{\mathbf{q}\lambda}$, cannot become positive in this case, which is, as we have already mentioned above, the hallmark of phonon vacuum squeezing in real space. In the above expression, \hbar is Planck's constant, M is the atomic mass of silver, and $\omega_{\mathbf{q}\lambda}$ is the frequency of a particular phonon mode. We note that the variance of the conjugate variable of $Q_{\mathbf{q}\lambda}$, the phonon momentum $P_{\mathbf{q}\lambda}$, which behaves oppositely, might squeeze below its 0K width following femtosecond-laser-induced bond softening.

Noble metals show, as we explained in Sec. II, laser-induced bond hardening, which is equivalent to a laser-modified potential that is narrower than the ground-state potential. For these materials, we shall demonstrate that the wave packet may initially squeeze in real space with $S > 0$, depending on the degree of phonon hardening and the incoherent rate of energy transfer from the hot electrons to the lattice, which are both functions of the excitation density.

For studying the possibility of vacuum squeezing in laser-excited silver, it is necessary to calculate the time-dependent variance of the *coherent* laser-induced atomic displacements in the direction of particular phonon modes quantum mechanically using [21]

$$\begin{aligned} \langle Q_{\mathbf{q}\lambda}^2(t) \rangle_{\text{coh}} &= \frac{\hbar M}{2} \sum_{\lambda'} \omega_{\mathbf{q}\lambda'} |\boldsymbol{\varepsilon}_{\mathbf{q}\lambda'}^e \cdot \boldsymbol{\varepsilon}_{\mathbf{q}\lambda}|^2 \\ &\times \left[\left(\frac{\cos \omega_{\mathbf{q}\lambda'}^e t}{\omega_{\mathbf{q}\lambda'}} \right)^2 + \left(\frac{\sin \omega_{\mathbf{q}\lambda'}^e t}{\omega_{\mathbf{q}\lambda}} \right)^2 \right], \end{aligned} \quad (3)$$

where $\omega_{\mathbf{q}\lambda}$ ($\omega_{\mathbf{q}\lambda}^e$) and $\boldsymbol{\varepsilon}_{\mathbf{q}\lambda}$ ($\boldsymbol{\varepsilon}_{\mathbf{q}\lambda}^e$) are, respectively, phonon frequencies and eigenvectors in the ground (laser-excited) state, which we calculated *ab initio* in the local density approximation [31] using the full-potential linearized augmented plane-wave code WIEN2k [32]. The $\omega_{\mathbf{q}\lambda}$ were determined from the second derivatives of the ground-state total energy computed along the phonon directions shown in the insets of Fig. 4 and the laser-excited phonon frequencies were obtained non-self-consistently [26] using

$$U(T_e) \approx U(0) + \Delta F_{\text{band}}, \quad (4)$$

where $\Delta F_{\text{band}} = \Delta E_{\text{band}} - T_e S_e$, $\Delta E_{\text{band}} = E_{\text{band}}(T_e) - E_{\text{band}}(0)$ is the laser-induced change in the band energy, and S_e is the electronic entropy. Typically, if $\omega_{\mathbf{q}\lambda}^e > \omega_{\mathbf{q}\lambda}$, the variance $\langle Q_{\mathbf{q}\lambda}^2(t) \rangle_{\text{coh}}$ will initially decrease after $t = 0$, which is the time of the laser excitation. We show our computed time-dependent variance of the coherent atomic displacements in the directions of two phonon modes in Fig. 4 (black curves).

IV. INCOHERENT ELECTRON-PHONON COUPLING

In addition to the coherent oscillations of Eq. (3), there is an incoherent heat transfer from the hot electrons to the lattice, which we approximated by simulating the evolution of the lattice and electronic temperatures, T_l and T_e , in laser-excited silver using the coupled equations of the generalized

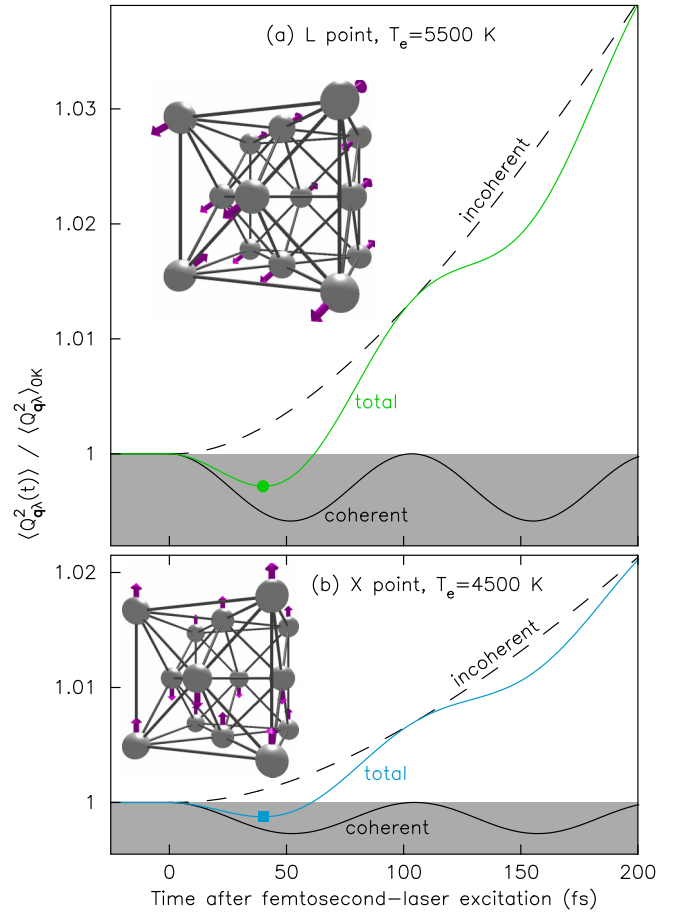


FIG. 4. (Color online) Normalized time-dependent variance of the atomic displacements (a) for the *L*-point (initial laser-induced $T_e = 5500$ K) and (b) for the *X*-point (initial laser-induced $T_e = 4500$ K) longitudinal phonon. The solid black curves show coherent phonon squeezing and the dashed black curves show incoherent lattice heating. The colored curves show the total variances. Filled symbols indicate the points of greatest squeezing. The shaded regions show the zero-point motion in the initial states. Insets: The directions of the atomic displacements in these two phonon modes.

two-temperature model (TTM) [27,33],

$$C_e \frac{\partial T_e}{\partial t} = -G(T_e - T_l), \quad (5)$$

$$C_l \frac{\partial T_l}{\partial t} = G(T_e - T_l), \quad (6)$$

where $C_l(T_l)$ and $C_e(T_e)$ are, respectively, the lattice and electronic heat capacities and $G(T_e)$ is the electron-phonon coupling factor. Note that C_e and G depend on the electronic temperature and C_l depends on the lattice temperature. Equations (5) and (6) consider only the temporal dependencies $T_l(t)$ and $T_e(t)$ and do not include their depth dependence, effectively describing noble metals in a thin-film geometry (see Ref. [34]). To solve the equations of the TTM, we computed the heat capacity of electrons, which we show in Fig. 5, from the Kohn-Sham eigenenergies. In order to obtain the phonon heat capacity, we computed the full phonon spectrum by diagonalizing the dynamical matrix of silver. We constructed

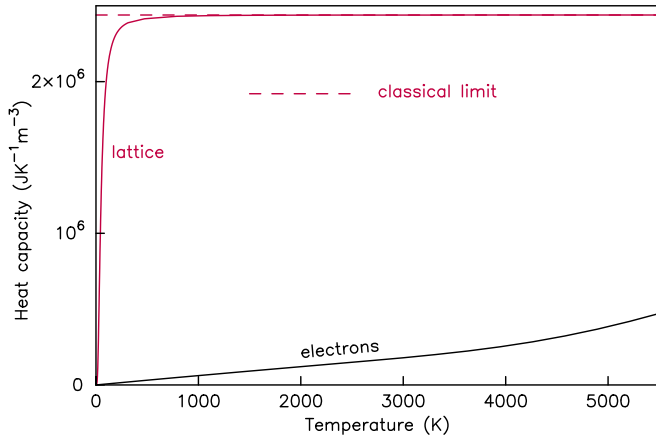


FIG. 5. (Color online) Computed electron and lattice heat capacities as a function of their respective temperatures. The dashed line indicates the classical limit of the phonon heat capacity, $3Nk_B$, with N the density of atoms per m^3 .

this matrix from the interatomic force constants up to the sixth nearest neighbors that we obtained by displacing one atom in a 32-atom supercell by a small distance and by computing the forces on the other 31 atoms as in Ref. [35]. We used the electron-phonon coupling data from Lin *et al.* [27,36]. We found that the lattice heats rather rapidly. For example, a particular laser excitation heating the electrons to 5500 K (the excitation density equals 1.00 GJ/m^3), whose effect we study in Fig. 4(a), heats the lattice to 124 K with an average heating rate of 0.12 K/fs during the first 1 ps, as shown in Fig. 6.

From the so-obtained time-dependent lattice temperature, we calculated the increase of the variance of phonons with quantum numbers $\{\mathbf{q}, \lambda\}$ due to incoherent lattice heating in the harmonic approximation to be [3]

$$\Delta \langle Q_{\mathbf{q}\lambda}^2(t) \rangle_{\text{incoh}} = \frac{\hbar}{2M\omega_{\mathbf{q}\lambda}^e} \left\{ \coth \left[\frac{\hbar\omega_{\mathbf{q}\lambda}^e}{2k_B T_l(t)} \right] - 1 \right\}, \quad (7)$$

as shown in Fig. 4 by the dashed curves. The total variance due to coherent squeezing and incoherent lattice heating is given

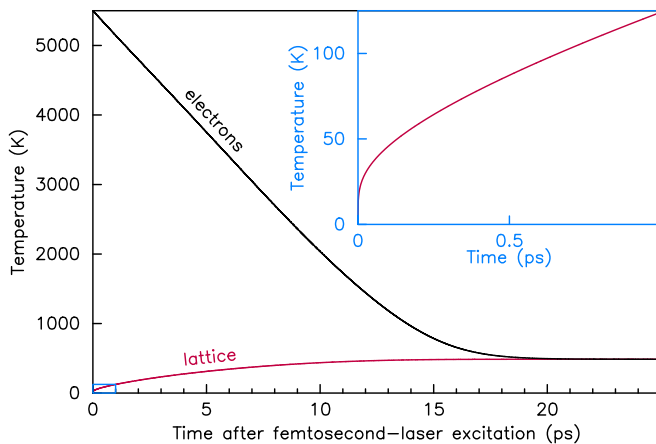


FIG. 6. (Color online) Evolution of electron and lattice temperatures after a laser excitation heating the electrons to 5500 K according to the generalized TTM. Inset: The indicated region enlarged.

by

$$\langle Q_{\mathbf{q}\lambda}^2(t) \rangle_{\text{tot}} = \langle Q_{\mathbf{q}\lambda}^2(t) \rangle_{\text{coh}} + \Delta \langle Q_{\mathbf{q}\lambda}^2(t) \rangle_{\text{incoh}}. \quad (8)$$

We note that the lattice heating leads to an increase of the mean-square atomic displacements counteracting the squeezing effect. As we will show below, our calculations indicate that a femtosecond-laser pulse can nevertheless transiently induce phonon vacuum squeezing.

V. PHONON VACUUM SQUEEZING

In Fig. 4 (colored curves), we show the total time-dependent variances of the atomic displacements in the directions of the L - and X -point longitudinal phonon modes immediately following an intense femtosecond-laser excitation [Eq. (8)] leading to $T_e = 5500$ and 4500 K , respectively. We see that immediately after the laser excitation, $\langle Q_{\mathbf{q}\lambda}^2(t) \rangle_{\text{tot}}$ dips below the zero-point motion (shaded regions in Fig. 4). The lowest values of $\langle Q_{\mathbf{q}\lambda}^2(t) \rangle_{\text{tot}}$ have been reached in both points 40 fs after the femtosecond-laser excitation and are denoted by filled symbols, which are the points with the greatest squeezing factors.

We repeated our simulations of femtosecond-laser-induced phonon squeezing for different excitation densities. Our resulting dependencies on the laser-induced electronic temperature of the maximal squeezing factors for silver at the L - and X -point longitudinal modes are shown in Fig. 7. We find that the squeezing factors increase with T_e up to a certain maximum value, after which they start to decrease. This decline is caused by the T_e dependencies of the electron-phonon coupling factor, which is nearly constant up to the temperature of $\sim 5000 \text{ K}$, and shows a significant strengthening at higher temperatures (see Fig. 2(d) in Ref. [27]). As mentioned above, vacuum squeezing in real space takes place only if $S > 0$. We found an optimal squeezing factor of 0.0014 at the L -point longitudinal mode at $T_e = 5500 \text{ K}$, which is small but nevertheless three orders of magnitude greater than the previously reported quantum squeezing in a transparent KTaO_3 crystal [2]. Our results therefore provide a strong indication that femtosecond-laser

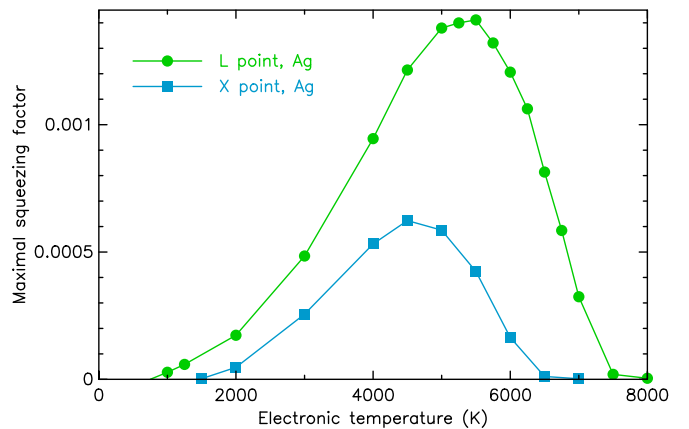


FIG. 7. (Color online) Maximal squeezing factor S of the L -point (green circles) and X -point (blue squares) longitudinal phonons for various laser fluences heating the electrons to different initial temperatures. The maximal squeezing effect reaches its optimum at laser fluences leading to $T_e = 5500$ and 4500 K , respectively.

excitation leads to transient phonon squeezing in opaque bond-hardening materials. From Figs. 4(a) and 4(b), it is clear that the total variance dips steeper below the zero-point motion for the L point than for the X point. In agreement, the greatest hardening occurs at the L point compared to other phonon wave vectors [35]. In addition to the ultrafast bond hardening, which is a necessary condition for the achievement of vacuum squeezing, it is important to realize that squeezing can only overcome the lattice heating if silver is excited by an ultrafast pulse clearly shorter than the time scale of phonon squeezing, i.e., below 40 fs.

VI. DISCUSSION

Previously, *ab initio* calculations have predicted that hardening of phonon modes in gold due to increased T_e results in an increase of the melting time [24,34], which provides already strong evidence of bond hardening. The observed delay in the melting time is small for aluminum, but has been shown to become large for gold [34]. We expect that such significant delay in melting should also be observable in silver. The conclusion that there is bond hardening on the basis of delayed melting relies, however, on electronic and lattice heat capacities and on the electron-phonon coupling parameter, which are calculated functions of the electronic excitation, and is therefore indirect. In contrast, the time-dependent variance of the atomic displacement is directly observable from the time-resolved diffraction intensities through structure factors using time-dependent Debye-Waller theory [21,34,37]. Recent progress in time-resolved diffuse x-ray scattering techniques permits one to explore the nonequilibrium lattice dynamics of particular phonon modes as well [22,38]. Measuring vacuum squeezing in real space by means of diffuse background scattering would thus provide direct evidence of bond hardening because the coherent part of the squeezing [Eq. (3)] depends only on the laser-modified potential.

We remark that the generalized TTM allowed us to calculate the temperatures of the electrons and phonons averaged over all \mathbf{q} vectors. However, the coupling strength of electrons with the lattice varies from point to point in the BZ and it is impossible to resolve a particular phonon mode using the TTM. In addition, 40 fs are far too short for reaching thermal equilibrium among the lattice degrees of freedom [3,38]. Consequently, at some points in the BZ, our approach based on the generalized TTM is bound to underestimate the effects of lattice heating, while at other points it may overestimate $\Delta\langle Q_{\mathbf{q}\lambda}^2(t)\rangle_{\text{incoh}}$. The fact that our results show that phonon vacuum squeezing can be induced at different points in the BZ of silver indicates that our conclusions are probably not overly sensitive to the approximations of the TTM, which provides the best currently available macroscopic description of incoherent lattice heating after femtosecond-laser excitation.

Our maximum predicted phonon vacuum squeezing factor in silver is of the order of 10^{-3} . Provided one could find materials with greater bond hardening or a smaller electron-phonon coupling factor, it might be possible to improve this result by one or two orders of magnitude. Based on their chemical and physical similarities, we expect that phonon vacuum squeezing can also be achieved in copper and gold.

ACKNOWLEDGMENTS

Financial support from the DFG (Grants No. GA 465/16-1 and No. ZI 1307/1-1), University of Kassel, and DAAD are gratefully acknowledged. Calculations were performed at the ITS, University of Kassel. We further thank Nadine Götte for various useful comments that helped us to improve the presentation of our results, Silvio Morgenstern and Marlene Adrian for suggesting the inset of Fig. 1, and Lucila Maitreya Juárez Reyes for general comments.

-
- [1] See, for example, W. P. Scheich, *Quantum Optics in Phase Space* (Wiley, Berlin, 2001).
 - [2] G. A. Garrett, A. G. Rojo, A. K. Sood, J. F. Whitaker, and R. Merlin, *Science* **275**, 1638 (1997).
 - [3] E. S. Zijlstra, A. Kalitsov, T. Zier, and M. E. Garcia, *Phys. Rev. X* **3**, 011005 (2013).
 - [4] Ö. E. Müstecapoglu and A. S. Shumovsky, *Appl. Phys. Lett.* **70**, 3489 (1997).
 - [5] H. Vahlbruch, M. Mehmet, S. Chelkowski, B. Hage, A. Franzen, N. Lastzka, S. Gossler, K. Danzmann, and R. Schnabel, *Phys. Rev. Lett.* **100**, 033602 (2008).
 - [6] H. P. Yuen and J. H. Shapiro, *IEEE Trans. Inf. Theory* **24**, 657 (1978).
 - [7] C. M. Caves, *Phys. Rev. D* **23**, 1693 (1981).
 - [8] See also the special issue on squeezed states: *Appl. Phys. B* **55**, No. 3 (1992).
 - [9] D. E. Reiter, S. Sauer, J. Huneke, T. Papenkort, T. Kuhn, A. Vagov, and V. M. Axt, *J. Phys.: Conf. Ser.* **193**, 012121 (2009).
 - [10] J. M. Daniels, T. Papenkort, D. E. Reiter, T. Kuhn, and V. M. Axt, *Phys. Rev. B* **84**, 165310 (2011).
 - [11] V. A. Kovarski, *Phys. Status Solidi B* **175**, K77 (1993).
 - [12] T. Papenkort, V. M. Axt, and T. Kuhn, *Phys. Rev. B* **85**, 235317 (2012).
 - [13] J. Janszky and An. V. Vinogradov, *Phys. Rev. Lett.* **64**, 2771 (1990).
 - [14] A. Žazunov, D. Feinberg, and T. Martin, *Phys. Rev. Lett.* **97**, 196801 (2006).
 - [15] M. Artoni and J. L. Birman, *Phys. Rev. B* **44**, 3736 (1991).
 - [16] X. Hu and F. Nori, *Phys. Rev. B* **53**, 2419 (1996).
 - [17] B. G. Levi, *Phys. Today* **50**, 18 (1997).
 - [18] D. A. Reis, *Physics* **2**, 33 (2009).
 - [19] X. Hu and F. Nori, *Phys. Rev. Lett.* **79**, 4605 (1997).
 - [20] G. A. Garrett, J. F. Whitaker, A. K. Sood, and R. Merlin, *Opt. Express* **1**, 385 (1997).
 - [21] S. L. Johnson, P. Beaud, E. Vorobeva, C. J. Milne, É. D. Murray, S. Fahy, and G. Ingold, *Phys. Rev. Lett.* **102**, 175503 (2009).
 - [22] M. Trigo, M. Fuchs, J. Chen, M. P. Jiang, M. Cammarata, S. Fahy, D. M. Fritz, K. Gaffney, S. Ghimire, A. Higginbotham, S. L. Johnson, M. E. Kozina, J. Larsson, H. Lemke, A. M. Lindenberg, G. Ndabashimiye, F. Quirin, K. Sokolowski-Tinten,

- C. Uher, G. Wang, J. S. Wark, D. Zhu, and D. A. Reis, *Nat. Phys.* **9**, 790 (2013).
- [23] E. S. Zijlstra, F. Cheenicode Kabeer, B. Bauerhenne, T. Zier, N. Grigoryan, and M. E. Garcia, *Appl. Phys. A* **110**, 519 (2013).
- [24] V. Recoules, J. Cl  rouin, G. Zerah, P. M. Anglade, and S. Mazevet, *Phys. Rev. Lett.* **96**, 055503 (2006).
- [25] M. Ligges, I. Rajkovic, P. Zhou, O. Posth, C. Hassel, G. Dumpich, and D. von der Linde, *Appl. Phys. Lett.* **94**, 101910 (2009).
- [26] N. S. Grigoryan, E. S. Zijlstra, and M. E. Garcia, *New J. Phys.* **16**, 013002 (2014).
- [27] Z. Lin, L. V. Zhigilei, and V. Celli, *Phys. Rev. B* **77**, 075133 (2008).
- [28] N. S. Grigoryan, E. S. Zijlstra, and M. E. Garcia (unpublished).
- [29]  . D. Murray, S. Fahy, D. Prendergast, T. Ogitsu, D. M. Fritz, and D. A. Reis, *Phys. Rev. B* **75**, 184301 (2007).
- [30] E. S. Zijlstra, L. E. D  az-S  nchez, and M. E. Garcia, *Phys. Rev. Lett.* **104**, 029601 (2010).
- [31] J. P. Perdew and Y. Wang, *Phys. Rev. B* **45**, 13244 (1992).
- [32] P. Blaha, K. Schwarz, G. K. H. Madsen, D. Kvasnicka, and J. Luitz, *WIEN2k, An Augmented Plane Wave + Local Orbitals Program for Calculating Crystal Properties* (Karlheinz Schwarz, Techn. Universit  t Wien, Austria, 2001).
- [33] S. I. Anisimov, B. L. Kapeliovich, and T. L. Perelman, *J. Exp. Theor. Phys.* **39**, 375 (1974).
- [34] R. Ernstorfer, M. Harb, C. T. Hebeisen, G. Sciaini, T. Dartigalongue, and R. J. Dwayne Miller, *Science* **323**, 1033 (2009).
- [35] F. Cheenicode Kabeer, E. S. Zijlstra, and M. E. Garcia, *Phys. Rev. B* **89**, 100301(R) (2014).
- [36] <http://www.faculty.virginia.edu/CompMat/electron-phonon-coupling> (unpublished).
- [37] S. L. Johnson, P. Beaud, E. Vorobeva, C. J. Milne,  . D. Murray, S. Fahy, and G. Ingold, *Acta Crystallogr. A* **66**, 157 (2010).
- [38] M. Trigo, J. Chen, V. H. Vishwanath, Y. M. Sheu, T. Graber, R. Henning, and D. A. Reis, *Phys. Rev. B* **82**, 235205 (2010).